Journal of Power Sources 196 (2011) 7601–7608

Contents lists available at ScienceDirect

Journal of Power Sources

journal homepage: www.elsevier.com/locate/jpowsour

Reducing the operation temperature of a solid oxide fuel cell using a conventional nickel-based cermet anode on dimethyl ether fuel through internal partial oxidation

Chao Su [a], Wei Wang [a], Huangang Shi [a], Ran Ran [a], Hee Jung Park [b], Chan Kwak [b,*], Zongping Shao [a,**]

[a] State Key Laboratory of Materials-Oriented Chemical Engineering, College of Chemistry & Chemical Engineering, Nanjing University of Technology, No. 5 Xin Mofan Road, Nanjing 210009, PR China
[b] Samsung Advanced Institute of Technology (SAIT), 14-1 Nongseo-dong, Yongin-si, Gyunggi-do 446712, Republic of Korea

ARTICLE INFO

Article history:
Received 1 March 2011
Received in revised form 25 April 2011
Accepted 26 April 2011
Available online 30 April 2011

Keywords:
Dimethyl ether
Solid-oxide fuel cells
Carbon deposition
Anode
Partial oxidation

ABSTRACT

Dimethyl ether (DME)-oxygen mixture as the fuel of an anode-supported SOFC with a conventional nickel-cermet anode for operating at reduced temperatures is systematically investigated. The results of the catalytic tests indicate that sintered Ni-YSZ has high activity for DME partial oxidation, and DME conversion exceeds 90% at temperatures higher than 700 °C. Maximum methane selectivity is reached at 700 °C. Cell performance is observed between 600 and 800 °C. Peak power densities of approximately 400 and 1400 mW cm^{-2} at 600 and 800 °C, respectively, are reached for the cell operating on DME-O_2 mixture. These values are comparable to those obtained using hydrogen as a fuel, and cell performance is reasonably stable at 700 °C for a test period of 340 min. SEM results demonstrate that the cell maintains good geometric integrity without any delimitation of respective layer after the stability test, and EDX results show that carbon deposition occurrs only at the outer surface of the anode. O_2-TPO analysis shows that carbon deposition over the Ni-YSZ operating on DME is greatly suppressed in the presence of oxygen. Internal partial oxidation may be a practical way to achieve high cell performance at intermediate-temperatures for SOFCs operating on DME fuel.

1. Introduction

The development of clean fuels and efficient energy conversion technologies is critical for a sustainable future. Dimethyl ether (DME) has the advantages of a high H/C ratio, high energy density, no toxicity and ease of storage and transportation. It can be produced from a wide range of primary fuels including natural gas, coal and biomass [1–3]. As a clean fuel, it is free of sulfur, heavy metals and other impurities. In addition, it has similar physical properties to those of liquefied petroleum gas (LPG); therefore, the existing liquid propane infrastructure can be easily transformed to handle, transport and store DME. It is believed that DME will play an important role in the energy supply systems of the future [4–6]. Fuel cells are a type of electrochemical energy conversion device with high efficiency and low emissions [7–9], which meet the requirements for future power sources. The use of DME in fuel cells is highly attractive because it combines the benefits of the environmental friendliness of DME fuel and the high efficiency of fuel cells [10–17].

Currently, most of the attention on DME in fuel cells has focused on the development of effective catalysts that produce hydrogen from DME, and some progress has been made in this regard [18–24]. Solid oxide fuel cells (SOFCs) are a type of high-temperature fuel cell that is fuel-flexible [25–30]. DME can be potentially directly fed into the anode of an SOFC without requiring an external reforming process [31,32]. This greatly simplifies fuel cell systems and increases overall fuel efficiency. Recently, DME as a fuel of SOFCs has attracted the attention of researchers [33–36].

In principle, SOFCs can operate on any fuel that is combustible. Cells with conventional nickel cermet anodes frequently encounter problems of low power output at intermediate temperatures and severe coke formation when operating directly on hydrocarbon fuels. In a previous study, we demonstrated that a state-of-the-art Ni-$(Y_2O_3)_{0.1}(ZrO_2)_{0.9}$ (YSZ) cermet anode catalyzed DME decomposition reactions and led to heavy carbon deposition [33]. Therefore, it is impractical to operate conventional SOFCs directly on pure DME fuel. Internal reforming can convert hydrocarbons to synthesis gas, which is a mixture of CO and H_2. Although the electro-oxidation rate of CO over nickel cermet anode is much slower

* Corresponding author. Tel.: +82 31 280 6721; fax: +82 31 280 6739.
** Corresponding author. Tel.: +86 25 83172256; fax: +86 25 83172242.
E-mail addresses: c.kwak@samsung.com (C. Kwak), shaozp@njut.edu.cn (Z. Shao).

0378-7753/$ – see front matter © 2011 Elsevier B.V. All rights reserved.
doi:10.1016/j.jpowsour.2011.04.056

than H_2, it was found that the cell delivers a similar power output when operating on a CO–H_2 gas mixture and pure hydrogen [37,38] because the water shift reaction occurs easily on the anode ($H_2O + CO = CO_2 + H_2$). Furthermore, internal reforming can suppress coke formation over the fuel cell anode due to the increased O to C molar ratio.

Previously, we demonstrated that the carbon deposition can be effectively suppressed at a temperature higher than 800 °C by introducing CO_2, which is the deep oxidation product of DME, into the fuel gas as a reforming gas. This is due to the high catalytic activity of the cermet anode for the CO_2 reforming of DME and methane (a decomposition product of DME) and the gasification of deposited solid carbon. However, the catalytic activity of the Ni-YSZ cermet for those three reactions was substantially reduced at a temperature lower than 800 °C and, as a result, coke formation on the anode became a serious problem again [33]. This implies that the operation of a cell on DME-CO_2 gas mixtures is possible only in a narrow temperature window of 800–850 °C.

At present, it is generally accepted that the wide implementation of SOFCs technology requires a decrease of the operation temperature to an intermediate temperature range of 500–800 °C. Compared to CO_2, O_2 is much more reactive and oxidative, which may be more effective in suppressing coke formation kinetically when operating on DME fuel, especially at a reduced temperature. By operating on a DME-O_2 gas mixture, the operating temperature can be further reduced below 800 °C. Recently, several studies have demonstrated that some catalysts possess high activity for DME partial oxidation at intermediate temperatures of 600–750 °C [22,23]. Therefore, it is possible to further reduce the operation temperature of SOFCs on DME fuel to lower than 800 °C through internal partial oxidation. The primary results reported by Murray strongly support this assumption [32].

In this study, we systematically investigated the potential operation of SOFCs with a conventional nickel cermet anode on DME-O_2 gas mixtures through internal partial oxidation. Cell performance with hydrogen fuel and the DME-O_2 (DME:O_2 = 2:1, volume ratio) gas mixture was comparatively studied at a temperature range of 600–800 °C. We paid special attention to the effect of oxygen on suppressing coke formation on the nickel cermet.

2. Experimental

The electrolyte material $(Y_2O_3)_{0.1}(ZrO_2)_{0.9}$ (YSZ) was purchased from Tosoh (Japan), and the composite cathode materials, including $Ba_{0.5}Sr_{0.5}Co_{0.8}Fe_{0.2}O_{3-\delta}$ (BSCF) and $Sm_{0.2}Ce_{0.8}O_{1.9}$ (SDC) oxide powders, were synthesized via a combined EDTA-citrate complexing sol–gel process [39]. The SDC oxide, which was used as a barrier layer, was obtained using the hydrothermal synthesis method [40].

This study used anode-supported cells with a configuration of (anode) Ni-YSZ | YSZ | SDC | BSCF-SDC (cathode). To fabricate the single cell, anode powders were first prepared by mixing NiO (Chengdu Shudu Nano-Science Co., Ltd., China) and YSZ in a weight ratio of 60:40, which was used for the fabrication of anode substrates by tape casting. After firing at 1100 °C for 2 h in air to remove organic solvents and create sufficient mechanical strength, the YSZ electrolyte layer was deposited onto the anode substrates via the wet powder spraying method. The NiO-YSZ | YSZ green disks were sintered at 1400 °C for 5 h in air, and then the SDC thin-film barrier layer was deposited onto the sintered YSZ electrolyte using the wet powder spraying method and fired at 1350 °C for 5 h. Finally, the BSCF-SDC (BSCF: SDC = 70: 30, by weight) composite cathode slurries were sprayed over the central surface of the SDC barrier layer via the spraying technique with a geometric surface area of 0.48 cm^2. It was then fired at 1000 °C for 2 h in air.

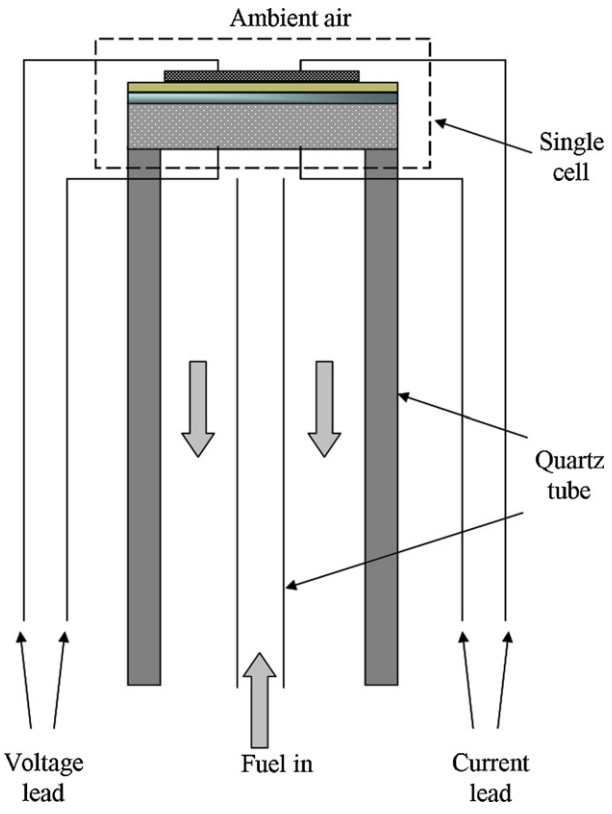

Fig. 1. The schematic diagram of the single cell test setup.

The partial oxidation of DME with and without the sintered Ni-YSZ cermet anode as a catalyst (at 1400 °C) was performed in a fixed-bed quartz tube reactor with an inner diameter of ~8 mm. Approximately 0.2 g of Ni-YSZ catalyst particles (after sintering at 1400 °C for 5 h), with a particle size of 40–60 mesh and that were diluted in 0.4 g inactive silica sand, were packed into the middle of the reactor to create a catalyst bed height of ~10 mm. For the blank reaction, 0.6 g inactive silica sand was put into the reactor to allow for a similar pressure drop as that of the catalytic test. A K-type thermocouple was inserted into the catalyst bed (or the quartz sand bed) to monitor and control the reaction temperature. Prior to the catalytic test, the catalyst was reduced by pure hydrogen at a flow rate of 40 mL min^{-1} [STP: standard temperature and pressure] at 850 °C for 1 h. After purging with argon gas for 10 min, the reactant gases, which were composed of DME, O_2 and He diluting gas, were fed into the reactor for the catalytic test. The flow rates of DME, O_2 and He were 10, 5, 80 mL min^{-1} [STP], respectively, and were controlled by three different AFC 80MD digital mass flow controllers (Qualiflow). The gases were well-mixed before entering the reactor. The reactions were performed at 450–850 °C. The water in the effluent gas was removed by passing through an anhydrous $CaCl_2$ adsorbent, and then the products were analyzed using an online gas chromatograph (CP-3800, VARIAN) that was equipped with a thermal conductivity detector (TCD), a Hayesep Q, a Poraplot Q and a 5 Å sieve molecular capillary columns for separating and detecting H_2, O_2, CO, CO_2 and CH_4, respectively, and a flame ionization detector (FID) for analyzing DME and CH_4.

Cell performance was tested in a home-built electrochemical work station. Fig. 1 illustrates the detailed configuration of the single cell test setup. The cell was sealed onto a quartz tube reactor using silver paste (DAD-87, Shanghai, China) with the cathode side exposed to ambient air while the anode chamber was swept with a DME-O_2 gas mixture or 3% water humidified hydrogen at a flow rate of 80 mL min^{-1} [STP]. The test temperature ranged from 600 °C

to 800 °C. The *I–V* polarization curves of the cells were collected by a digital sourcemeter (Keithley 2420, USA) that was based on a four-probe configuration. Electrode performance was determined by a complete cell configuration, and the electrochemical impedance spectroscopy (EIS) of the cells was measured under open circuit voltage (OCV) or a constant voltage polarization of 0.7 V conditions using a Solartron 1260 Frequency Response Analyzer combined with a Solartron 1287 potentiostat. The frequency ranged from 0.1 to 1000 kHz, and the signal amplitude was 20 mV.

To test the coke resistance of the Ni-YSZ anode, approximately 0.2 g of Ni-YSZ powder that was sintered at 1400 °C for 5 h was placed into a flow-through quartz tube reactor with an inner diameter of ~8 mm and treated in the DME-O_2 gas mixture (DME:O_2 = 2:1, volume ratio) with a constant DME flow rate of 40 ml min^{-1} [STP] at selected temperatures (800, 750, 700, 650 or 600 °C) for 30 min. Then, the reactor was quickly cooled down to room temperature by removing the reactor from the furnace instantly and placing it in an atmosphere of pure helium. Next, approximately 0.02 g of the treated sample was placed into a U-type quartz reactor with an inner diameter of ~3 mm, and 10 vol.% O_2–Ar gas mixture at a flow rate of 20 ml min^{-1} [STP] was introduced to the reactor for the oxygen temperature programmed oxidation (O_2-TPO) analysis. After flowing with gas at room temperature for 30 min to remove any weakly adsorbed surface species, the reactor was heated to 900 °C at a rate of 10 °C min^{-1}. During the programmatic increase in temperature, the carbon deposited on the Ni-YSZ was progressively oxidized to CO_2, which was analyzed on-line using a Hiden QIC-20 mass spectrometer (MS).

The microscopic features of the fuel cells from a cross-sectional view were examined using an environmental scanning electron microscope (ESEM, Quanta-200). The elemental distribution in the electrodes were analyzed by field emission scanning electron microscopy (FESEM, Hitachi S-4800) equipped with an energy dispersive X-ray analyzer (EDX).

3. Results and discussion

3.1. Non-catalytic and catalytic reaction between DME and O_2

It is believed that the electro-oxidation of DME over an SOFC anode proceeds via an indirect pathway by first converting to CH_4, CO and H_2. To achieve a high cell power output, the reactions towards CO and H_2 are preferred, whereas reactions towards methane and other hydrocarbons or oxygenated-hydrocarbons should be suppressed because the oxidation rate of hydrocarbons and oxygenated-hydrocarbons over a fuel cell anode is much less than H_2 and the H_2–CO gas mixture. Thermodynamically, coke formation is determined by the oxygen-to-carbon molar ratio in the reactants and the operation temperature; however, the actual amount of carbon that is deposited over the catalyst is also closely related to the reaction pathway.

By using a DME-O_2 mixture as the fuel gas, both the non-catalytic gas phase reaction and the catalytic partial oxidation over the fuel cell anode can occur within the anode chamber at the operating temperature. For both types of reactions, we found that CH_4, CO, CO_2, H_2 and H_2O are the main gaseous products. The possible chemical reaction formulas for the partial oxidation of DME are as follows.

$$CH_3OCH_3 \rightarrow H_2 + CO + CH_4 + CO_2$$

$$CH_4 + O_2 \rightarrow H_2 + CO + CO_2 + H_2O$$

$$CH_4 + H_2O \rightarrow H_2 + CO + CO_2$$

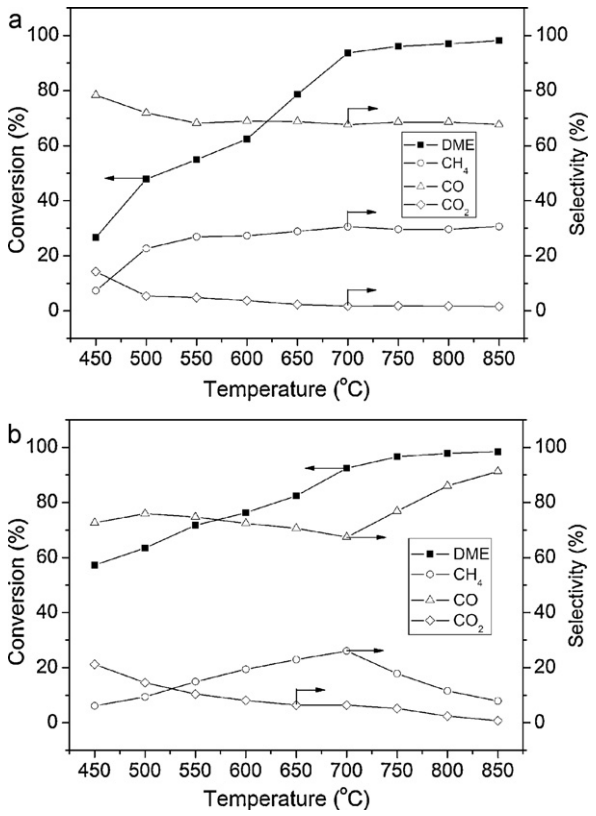

Fig. 2. The partial oxidation of DME without the catalyst (a) and with the Ni-YSZ catalyst (b).

$$CH_4 + CO_2 \rightarrow H_2 + CO + H_2O$$

$$CO_2 + H_2 \leftrightarrow CO + H_2O$$

The overall reaction is:

$$CH_3OCH_3 + O_2 \rightarrow CO + H_2 + CH_4 + CO_2 + H_2O$$

The ΔH of the partial oxidation of DME reaction is -74.065 kJ mol^{-1} at 25 °C, and the value is -34.970 kJ mol^{-1} at the operation temperature of 800 °C, and not high. Some endothermic reactions, such as CH_4 steam and CO_2 reforming, accompany with the partial oxidation of DME reaction, which help keeping the heat in balance. It indicated that DME-O_2 mixture could be used as the fuel for SOFC.

Fig. 2a and b shows the temperature dependence of DME conversion and CH_4, CO and CO_2 selectivity without and with the presence of the Ni-YSZ cermet anode catalyst, respectively, within the investigated temperature range of 450–850 °C. High DME conversion was observed even without the presence of the Ni-YSZ catalyst, and it reached 60% at 600 °C and increased to 96% at 800 °C. Previously, we demonstrated that pure DME has a relatively high thermal stability with a DME conversion of less than 2% at 600 °C and 20% at 800 °C by thermal decomposition. It is clear that the presence of oxygen promoted the decomposition of DME. Recently, Murray et al. demonstrated by kinetic modeling and a mass spectroscopy examination that oxygen can promote the decomposition of DME into primarily H_2, CO and CH_4 [32]. The promoting effect is due to the reduced activation energy (E_a) that is required for DME decomposition in the presence of oxygen. For example, the E_a for the extraction of an H atom from DME ($CH_3OCH_3 + O_2 = CH_3OCH_2 + HO_2$) is 188 kJ mol^{-1}, but it is as

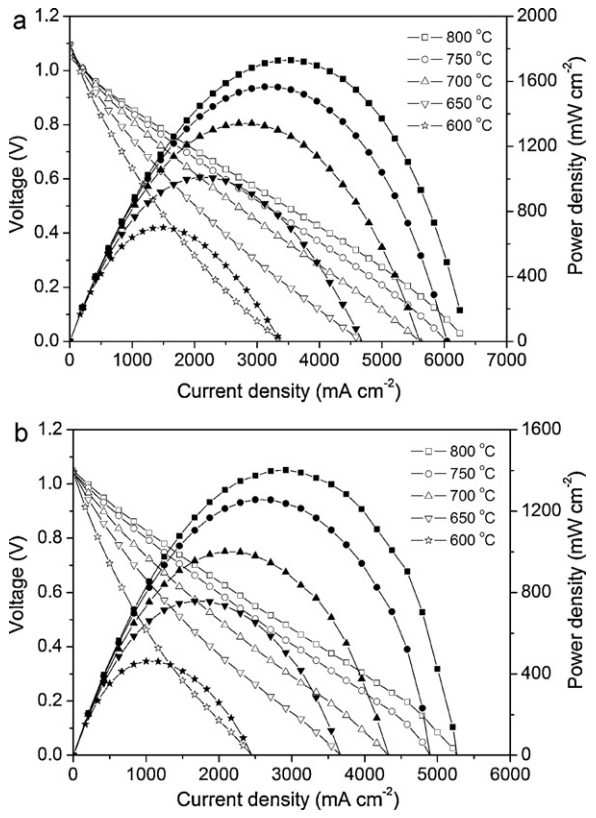

Fig. 3. The *I–V* and *I–P* polarization curves of the cell Ni-YSZ | YSZ | SDC | BSCF-SDC operating on hydrogen (a) and DME-O_2 gas mixtures (DME:O_2 = 2:1) (b) at various temperatures.

high as 426 kJ mol^{-1} for the unimolecular decomposition of DME (CH_3OCH_3=CH_3 + CH_3O).

As shown in Fig. 2a, a large amount of methane was formed by the gas phase reaction, and methane selectivity increased with a decrease of the reaction temperature from 850 to 700 °C. It reached its maximum at 700 °C, and then it decreased with the decrease of the reaction temperatures from 700 to 450 °C. The above results indicate that the actual gases approaching the anode are mainly composed of CH_4, CO_2, CO and H_2, and H_2O when applying DME and oxygen as the feed gas. Fig. 2b shows that the DME conversions were 97 and 76% at 800 °C and 600 °C, respectively, when Ni-YSZ catalyst was applied. DME conversion was 57% even at 450 °C, which was much higher than the conversion without the catalyst (26%). The above results indicate that the Ni-YSZ catalyst dramatically improved DME conversion at lower temperatures. Because the electrochemical oxidation rate of methane is much slower than hydrogen, the reaction towards methane is not favored for the following power generation. It is interesting to note that methane selectivity also had a maximum at 700 °C for the DME partial oxidation reaction under the catalysis of the Ni-YSZ cermet. However, methane selectivity in the presence of the Ni-YSZ catalyst was relatively lower than that without the catalyst. For example, it was 8% and 30% at 850 °C with and without the Ni-YSZ catalyst, respectively. This further suggested that the nickel cermet anode enhanced the methane partial oxidation and reforming reaction.

3.2. Cell performance

An anode-supported single cell with a configuration of (anode) Ni-YSZ | YSZ | SDC | BSCF-SDC (cathode) was used for the cell performance test. Fig. 3 shows the *I–V* and *I–P* polarization curves of the fuel cells operating on hydrogen and DME-O_2 (DME:O_2 = 2:1, volume ratio) fuel gases at temperatures between 600 and 800 °C. The corresponding EIS under OCV or a constant polarization voltage of 0.7 V conditions are shown in Fig. 4. The linear response of the cell voltage to the applied current density, even at high current density, indicates that concentration polarization did not occur for this cell, which operated on both hydrogen and DME-O_2 fuel gases. This could be explained by the high porosity of the electrodes that allowed for the free diffusion of the reaction gas and products within the electrode (this will be discussed later). As shown in Fig. 3a, favorable peak power densities of ~600 and 1800 mW cm^{-2} were achieved at 600 and 800 °C, respectively. It is well known that the BSCF possesses excellent catalytic activity for oxygen reduction at intermediate temperatures. However, the interfacial reaction between the BSCF and the YSZ electrolyte is a serious problem. By using an SDC barrier layer, the interfacial reaction between BSCF and YSZ was effectively suppressed; as a result, a very high power output was achieved for hydrogen fuel. By using the DME-O_2 mixture as the fuel gas, cell peak power density still reached ~400 and ~1400 mW cm^{-2} at 600 and 800 °C, respectively, as shown in Fig. 3b. The power output was a bit lower than that operating on H_2 at a corresponding temperature. This is because H_2 and CO were the main products for the catalytic partial oxidation of DME, and the concentration of H_2 in the fuel gas when DME-O_2 mixture as fuel is lower than that of pure H_2 fuel under the same flow rate. Fig. 4a and b shows that the electrode polarization resistances are comparable by using H_2 and DME-O_2 as fuels under a constant polarization voltage of 0.7 V at corresponding operating temperatures. Interestingly, under open circuit conditions, the electrode polarization resistance of the cell operating on the DME-O_2 gas mixture was much larger than that of the one on H_2 as shown in Fig. 4c and d. This is because DME was not fully converted to H_2 and CO under OCV conditions; therefore, the concentration of DME increased in the anode chamber, which led to an increase in electrode resistance. When the cell was polarized at a constant voltage of 0.7 V, a large amount of O^{2-} was transferred from the cathode through the electrolyte to the anode, and DME was almost completely converted to H_2 and CO on the anode surface; consequently, the electrode resistance of the cell was significantly reduced.

Performance stability is an important concern for SOFCs operating on hydrocarbon fuels. In our previous work, we found an obvious degradation of cell performance after operating on pure DME under a constant polarization current density of 1000 mA cm^{-2} at 850 °C for 300 min for an anode-supported SOFC with a conventional nickel cermet anode [33]. The performance stability at 700 °C for the cell operating on the DME-O_2 gas mixture was also tested in this study. During the stability test, the volume ratio of DME to oxygen was 2:1, and the DME feed rate was set to 40 mL min^{-1} [STP]. Because many factors can lead to cell performance degradation, for a reasonable comparison, the operational stability of a similar cell on hydrogen fuel was also investigated. The cell was polarized under a constant current density of 1000 mA cm^{-2} when operating on H_2, but it was fixed at 625 mA cm^{-2} when operating on DME-O_2 fuel to ensure a similar polarization voltage of ~0.7 V. As shown in Fig. 5, the cell voltage was relatively stable and decreased only slightly from an initial value of 0.71 to 0.70 V after the operation on hydrogen for a period of 340 min. When operating on the DME-O_2 gas mixture, cell voltage also decreased only slightly from an initial value of 0.73 V to 0.71 V after operation for a period of 340 min. This indicates that cell performance was nearly stable when operating on the DME-O_2 gas mixture.

After the performance stability test of the cell operating on the DME-O_2 gas mixture at 700 °C was complete, the cell was slowly cooled down to room temperature under OCV conditions with the protection of anode by hydrogen atmosphere. Fig. 6 shows a digital picture of the anode surface after operating on the DME-O_2 gas

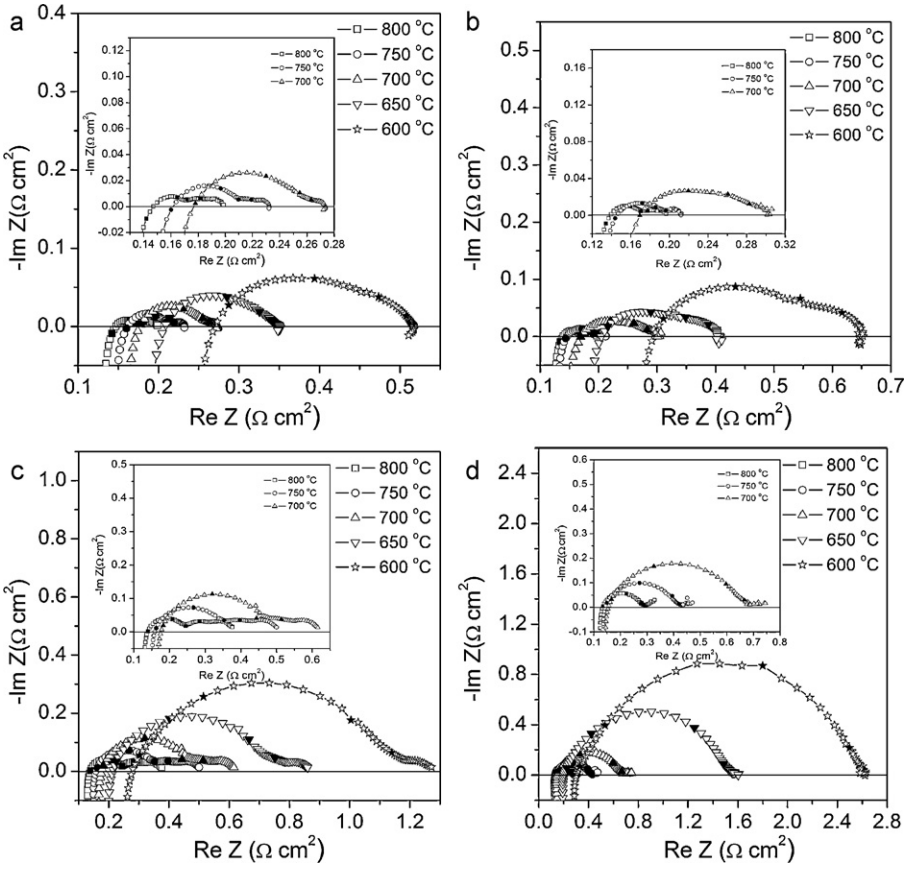

Fig. 4. The impedance spectra of the cell Ni-YSZ | YSZ | SDC | BSCF-SDC operating on hydrogen (a and c) and DME-O_2 gas mixtures (DME:O_2 = 2:1) (b and d) at different temperatures under a constant voltage of 0.7 V (a and b) and OCV (c and d) conditions. The four representative frequencies of 10,000, 1000, 100 and 10 Hz in each curve are marked with solid points from high to low frequency.

mixture. A dark coating was observed on the Ni-YSZ anode surface. This implies that coke likely formed after the stability test. It is well known that carbon deposited on the anode active sites decreases cell performance, and too much carbon deposition on the anode can cause the fuel cell to fail by destroying the geometric integrity of the cell. However, as shown in Fig. 6, no cracks formed on the fuel cell. This suggests that the cell maintained sound geometric integrity after the stability test. To further exploit carbon formation behavior on the anode, after the stability test, the single cell was investigated by SEM-EDX. Fig. 7 shows the SEM morphology of the four-layer cell in a cross-sectional view. Porous electrodes and dense electrolyte morphology were clearly demonstrated, which ensure high cell performance. No delimitation of the cell components was observed, which further indicates that carbon deposition did not destroy or impair the geometric integrity of the fuel cell. Carbon deposition on the anode was further analyzed using EDX. As shown in Fig. 8, Regions 1, 2, 3 and 4 represented the selected locations within the YSZ electrolyte, within the electrolyte–anode interface, within the anode and within the anode near the surface, respectively. In principle, there should be no carbon deposited over the dense electrolyte from DME decomposition because it could not reach the electrolyte. However, a weak carbon peak was detected by EDX on the electrolyte layer as shown in Fig. 8a. This carbon may have come from contamination when the sample was being prepared for EDX analysis. The weight ratio of contaminated carbon in Region 1 was approximately 22.8 wt.%. As shown in Fig. 8b and c, the amounts of carbon in Regions 2 and 3 were 20.7 and 28.6 wt.%, respectively, which was similar to the amount of contaminated carbon found in Region 1. This implies that there was almost no carbon deposited due to DME decomposition inside the anode after operation on the DME-O_2 fuel gas. In Region 4, i.e., the location near the anode's outer surface, the intensity of the carbon peak increased significantly as compared to that in Regions 1–3, and the amount of carbon reached 52.6 wt.%; this is shown in Fig. 8d. Based on the above-mentioned results, carbon deposition occurred only at the outer surface of the anode when operating on the DME-O_2 gas mixture. It is well-known that the active sites in an electrode located on the narrow regions close to the electrolyte have a thickness of only tens of micrometers [41]. The SEM-EDX analysis showed that no coke formation occurred in those active regions, which explains the relatively stable performance of a cell operating on the DME-O_2 gas mixture.

3.3. Carbon deposition behavior

In a previous study, we demonstrated that carbon deposition on the traditional Ni-YSZ anode of an SOFC was serious when pure DME was used as fuel [33], because the Ni-YSZ cermet can catalyze the decomposition of DME with the formation of coke over the anode. A large amount of carbon deposition can damage the anode structure, which affects cell performance. Based on the above-mentioned SEM-EDX analysis, the carbon was only deposited over the anode's outer surface after operation for a relatively short period of 340 min. However, for practical applications, the fuel cell must be operated for much longer time period. To further examine the coke formation behavior of the anode operating on DME-O_2 fuel gas, the Ni-YSZ anode material was treated in the DME-O_2 gas mixture at different temperatures for 30 min under OCV conditions, and O_2-TPO analysis was performed. Fig. 9 presents the O_2-TPO profiles with CO_2 signals. The amount of deposited carbon on the Ni-YSZ

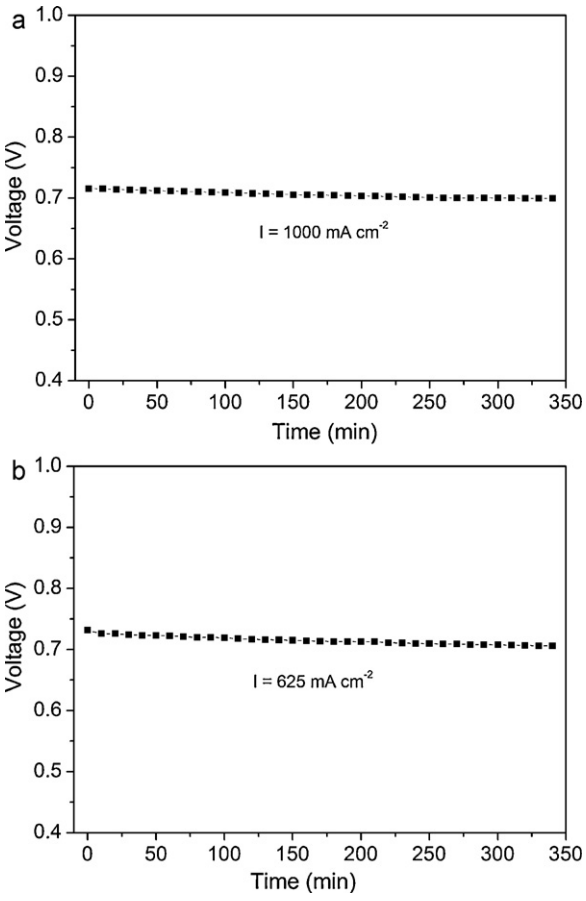

Fig. 5. Time dependence of the polarization curve of Ni-YSZ anode in a hydrogen atmosphere (a) and DME-O_2 gas mixtures (b) under a constant polarization current at 700 °C.

powder that was treated under a DME-O_2 atmosphere was much less than the one treated in a pure DME atmosphere for the same time period of 30 min [33]. In particular, carbon deposition was suppressed effectively at temperatures below 650 °C. The CO_2 peak areas for the Ni-YSZ anode after treatment in the DME-O_2 gas mixture at 800, 750, 700, 650 and 600 °C were 0.43×10^{-6}, 1.04×10^{-6}, 2.77×10^{-6}, 1.50×10^{-6} and 0.71×10^{-6}, respectively, whereas they were 4.77×10^{-6}, 3.51×10^{-6}, 2.99×10^{-6} and 2.51×10^{-6} for the Ni-YSZ anode after the treatment in pure DME for the same time

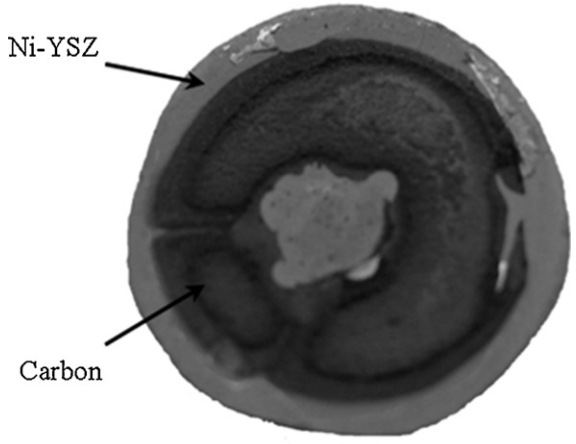

Fig. 6. A digital photo of the anode surface of the cell Ni-YSZ | YSZ | SDC | BSCF-SDC after operating on DME-O_2.

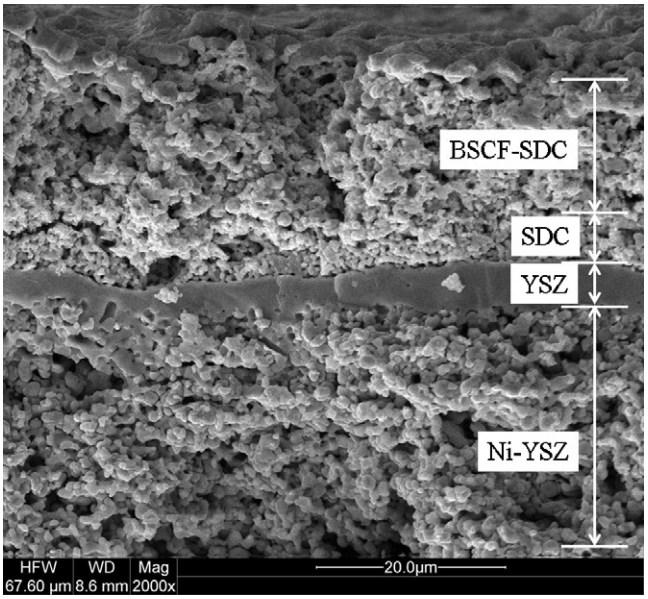

Fig. 7. SEM photo of the cell Ni-YSZ | YSZ | SDC | BSCF-SDC after operating on DME-O_2.

period at 800, 750, 700 and 650 °C, respectively [33]. It is interesting that the amount of deposited carbon increased with temperature, reaching a maximum at 700 °C, and then decreased with the further increase in operating temperature. This trend is the same as the one for methane selectivity, which implies that coke formation is mainly due to methane decomposition.

To further observe and assess coke formation in an actual fuel cell operating on a DME-O_2 gas mixture under OCV conditions, five identical single cells with a Ni-YSZ anode (the diameter of the cells were all about 12.51 mm) were treated with the DME-O_2 gas mixture (DME:O_2 = 2:1, volume ratio) at various temperatures (800, 750, 700, 650 and 600 °C) for a period of 30 min. During treatment, the DME flow rate was maintained at 40 ml min^{-1} [STP]. Fig. 10 shows the digital photos of a fresh cell and the cells after treatment in the DME-O_2 atmosphere at various temperatures, which are displayed from the anode side. In our previous work, severe damage to the Ni-YSZ anode disks was observed when the cells were treated in pure DME, especially at temperatures lower than 750 °C [33]. However, as shown in Fig. 10, no obvious deformation was found in all of the cells after treatment in DME-O_2, and a small amount of black carbon was detected on the anode surface for the cells treated between 600 and 700 °C. The weight gain and diameter changes of the cells after treatment in DME-O_2 at various temperatures are listed in Table 1. The weight of the cells after treatment at 800 and 750 °C increased by only 0.43 and 2.6%, respectively, whereas only a minimal change was observed in the size of the cells. Clearly, both the weight and the size changes originated due to coke formation on the anode. In connection with our previous results for cells treated on pure DME [33], carbon deposition was effectively suppressed by introducing O_2 into the DME fuel gas. The cell that was treated at 700 °C showed the largest size expansion (10%) among the treated cells, which agreed well with the fact that coke formation was the most severe at 700 °C when operating on DME-O_2 fuel gas.

Under current polarization, additional oxygen was diffused from the cathode side to the anode side; as a result, the oxygen-to-carbon ratio increased, which effectively suppressed coke formation over the anode thermodynamically. As a result, under actual fuel cell operation conditions (under polarization), less severe coke formation over the fuel cell anode was detected as shown in the previous section.

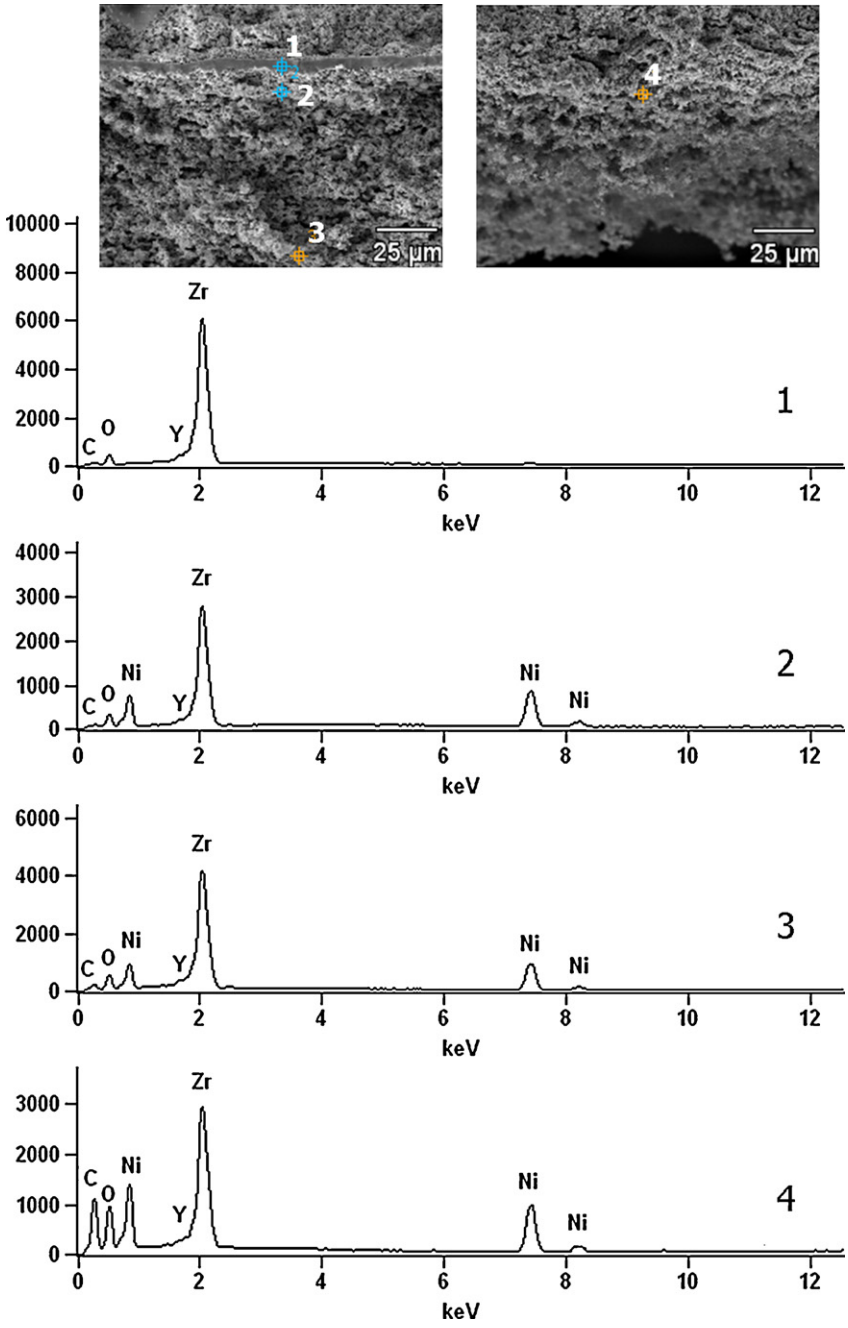

Fig. 8. EDX profiles of the cell Ni-YSZ | YSZ | SDC | BSCF-SDC after operating on DME-O_2.

Table 1
The weight and diameter differences between the fresh cell and the cell after the treatment in DME-O_2 at various temperatures.

Temperature (°C)	m_f (g)[a]	m_t (g)[b]	100 (m_t–m_f)/m_f (%)	d_f (mm)[c]	d_t (mm)[d]	100 (d_t–d_f)/d_f (%)
800	0.4467	0.4486	0.43	12.51	12.57	0.48
750	0.4437	0.4552	2.6	12.51	12.60	0.72
700	0.4550	0.5003	10.0	12.51	13.55	8.3
650	0.4628	0.4949	6.9	12.51	13.18	5.4
600	0.4664	0.4904	5.1	12.51	13.03	4.2

[a] Weight of the fresh cell.
[b] Weight of the cell after the treatment in DME-O_2 gas mixtures.
[c] Diameter of the fresh cell.
[d] Diameter of the cell after the treatment in DME-O_2 gas mixtures.

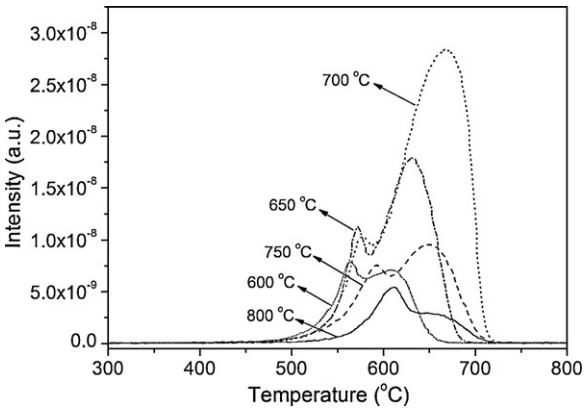

Fig. 9. O_2-TPO profiles of Ni-YSZ after treatment in DME-O_2 for 30 min at various temperatures.

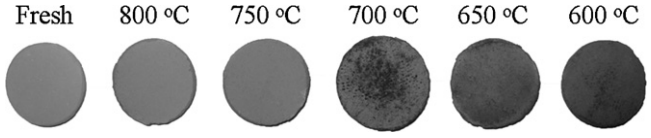

Fig. 10. Digital photos of the fresh anode and the anodes after treatment in DME-O_2 gas mixtures (DME:O_2 = 2:1) for 30 min at various temperatures.

4. Conclusions

Oxygen promoted DME decomposition both with and without the Ni-YSZ cermet anode at intermediate temperatures. In particular, the Ni-YSZ anode catalyst showed excellent catalytic activity for DME partial oxidation with DME conversion reaching 57% even at 450 °C. The main products of the reaction between DME and O_2 are CO, H_2, CH_4, H_2O and CO_2. Methane is not favored due to the low oxidation rate over the anode. Methane selectivity reached a maximum at 700 °C both with and without a Ni-YSZ catalyst. The good catalytic activity of Ni-YSZ for DME partial oxidation resulted in high cell performance when the SOFC was operated on DME-O_2 at intermediate temperatures with peak power densities that were comparable to operation on hydrogen fuel even at 700 °C. The performance of the cell operating on the DME-O_2 fuel gas under current polarization for a test period of 340 min at 700 °C was reasonably stable. Although carbon deposition did occur on the anode's outer surface after the stability test, coke formation was greatly suppressed in the presence of oxygen. No carbon was formed inside the anode layer, which ensured stable cell performance. Maximum carbon deposition was found are approximately 700 °C for the anode operating on DME-O_2 fuel (2:1 volume ratio); therefore, the elimination of deposited carbon at 700 °C is the next major challenge. The results of present study suggest that the operation temperature of a SOFC operating on DME fuel can be effectively reduced to lower than 800 °C through internal partial oxidation.

Acknowledgements

This work was supported by the National Basic Research Program of China under contract No. 2007CB209704, the National Science Foundation for Distinguished Young Scholars of China under contract No. 51025209, the program for New Century Excellent Talents (2008) and the Fok Ying Tung Education Foundation under contract No. 111073. This work was also supported by the Development of Innovative Anode and Cathode Materials for SOFC Towards Reduced Temperature Operation, SAIT, Samsung Electronics Co., Ltd., Korea.

References

[1] W. Cho, T. Song, A. Mitsos, J.T. McKinnon, G.H. Ko, J.E. Tolsma, D. Denholm, T. Park, Catal. Today 139 (2009) 261–267.
[2] L. Zhou, S.Y. Hu, Y.R. Li, Q.H. Zhou, Chem. Eng. J. 136 (2008) 31–40.
[3] F.D. Ju, H.P. Chen, X.J. Ding, H.P. Yang, X.H. Wang, S.H. Zhang, Z.H. Dai, Biotechnol. Adv. 27 (2009) 599–605.
[4] T.H. Fleisch, A. Basu, M.J. Gradassi, J.G. Masin, Stud. Surf. Sci. Catal. 107 (1997) 117–125.
[5] T.A. Semelsberger, R.L. Borup, H.L. Greene, J. Power Sources 156 (2006) 497–511.
[6] C. Arcoumanis, C. Bae, R. Crookes, E. Kinoshita, Fuel 87 (2008) 1014–1030.
[7] B.C.H. Steele, A. Heinzel, Nature 414 (2001) 345–352.
[8] S.M. Haile, Acta Mater. 51 (2003) 5981–6000.
[9] C.K. Dyer, Nature 343 (1990) 547–548.
[10] I. Mizutani, Y. Liu, S. Mitsushima, K.-I. Ota, N. Kamiya, J. Power Sources 156 (2006) 183–189.
[11] J.H. Yoo, H.G. Choi, C.H. Chung, S.M. Cho, J. Power Sources 163 (2006) 103–106.
[12] K.D. Cai, G.P. Yin, J.J. Wang, L.L. Lu, Energy Fuels 23 (2009) 903–907.
[13] K. Xu, S.J. Lao, H.Y. Qin, B.H. Liu, Z.P. Li, J. Power Sources 195 (2010) 5606–5609.
[14] J.R. Ferrell III, M.C. Kuo, A.M. Herring, J. Power Sources 195 (2010) 39–45.
[15] J.-H. Yu, H.-G. Choi, S.M. Cho, Electrochem. Commun. 7 (2005) 1385–1388.
[16] S.Z. Wang, J. Gao, Electrochem. Solid-State Lett. 9 (2006) A395–A398.
[17] D. Cocco, V. Tola, Energy 34 (2009) 2124–2130.
[18] K. Takeishi, H. Suzuki, Appl. Catal., A 260 (2004) 111–117.
[19] K. Faungnawakij, Y. Tanaka, N. Shimoda, T. Fukunaga, R. Kikuchi, K. Eguchi, Appl. Catal. B 74 (2007) 144–151.
[20] X.L. Wang, X.M. Pan, R. Lin, S.Y. Kou, W.B. Zou, J.-X. Ma, Int. J. Hydrogen Energy 35 (2010) 4060–4068.
[21] S.D. Badmaev, P.V. Snytnikov, Int. J. Hydrogen Energy 33 (2008) 3026–3030.
[22] Q.J. Zhang, X.H. Li, K. Fujimoto, K. Asami, Appl. Catal. A 288 (2005) 169–174.
[23] Y.Z. Chen, Z.P. Shao, N.P. Xu, J. Nat. Gas Chem. 17 (2008) 75–80.
[24] S.Z. Wang, T. Ishihara, Y. Takita, Appl. Catal. A 228 (2002) 167–176.
[25] R.M. Ormerod, Chem. Soc. Rev. 32 (2003) 17–28.
[26] S. Park, J.M. Vohs, R.J. Gorte, Nature 404 (2000) 265–267.
[27] W. Wang, C. Su, R. Ran, Z.P. Shao, J. Power Sources 196 (2011) 3855–3862.
[28] C. Su, Y.Z. Wu, W. Wang, Y. Zheng, R. Ran, Z.P. Shao, J. Power Sources 195 (2010) 1333–1343.
[29] Y.Z. Wu, C. Su, C.M. Zhang, R. Ran, Z.P. Shao, Electrochem. Commun. 11 (2009) 1265–1268.
[30] A. Wojcik, H. Middleton, I. Damopoulos, J. Van herle, J. Power Sources 118 (2003) 342–348.
[31] E.P. Murray, S.J. Harris, H. Jen, J. Electrochem. Soc. 149 (2002) A1127–A1131.
[32] E.P. Murray, S.J. Harris, J. Liu, S.A. Barnett, Electrochem. Solid-State Lett. 8 (2005) A531–A533.
[33] C. Su, R. Ran, W. Wang, Z.P. Shao, J. Power Sources 196 (2011) 1967–1974.
[34] N. Laosiripojana, S. Assabumrungrat, Appl. Catal. A 320 (2007) 105–113.
[35] M. Yano, T. Kawai, K. Okamoto, M. Nagao, M. Sano, A. Tomita, T. Hibino, J. Electrochem. Soc. 154 (2007) B865–B870.
[36] S.Z. Wang, T. Ishihara, Y. Takita, Electrochem. Solid-State Lett. 5 (2002) A177–A180.
[37] Y. Jiang, A.V. Virkar, J. Electrochem. Soc. 150 (2003) A942–A951.
[38] A.M. Sukeshini, B. Habibzadeh, B.P. Becker, C.A. Stoltz, B.W. Eichhorn, G.S. Jackson, J. Electrochem. Soc. 153 (2006) A705–A715.
[39] H.X. Gu, R. Ran, W. Zhou, Z.P. Shao, J. Power Sources 172 (2007) 704–712.
[40] H.G. Shi, W. Zhou, R. Ran, Z.P. Shao, J. Power Sources 195 (2010) 393–401.
[41] S.X. Liu, W. Kong, Z.J. Lin, Energies 2 (2009) 427–444.